The Journal of Immunology

RESEARCH ARTICLE | JANUARY 01 2006

An Engineered Human IgG1 Antibody with Longer Serum Half-Life FREE

Paul R. Hinton; ... et. al

J Immunol (2006) 176 (1): 346–356.
https://doi.org/10.4049/jimmunol.176.1.346

An Engineered Human IgG1 Antibody with Longer Serum Half-Life

Paul R. Hinton,[1] Joanna M. Xiong, Mary G. Johlfs,[2] Meina Tao Tang, Stephen Keller, and Naoya Tsurushita

The serum half-life of IgG Abs is regulated by the neonatal Fc receptor (FcRn). By binding to FcRn in endosomes, IgG Abs are salvaged from lysosomal degradation and recycled to the circulation. Several studies have demonstrated a correlation between the binding affinity of IgG Abs to FcRn and their serum half-lives in mice, including engineered Ab fragments with longer serum half-lives. Our recent study extended this correlation to human IgG2 Ab variants in primates. In the current study, several human IgG1 mutants with increased binding affinity to human FcRn at pH 6.0 were generated that retained pH-dependent release. A pharmacokinetics study in rhesus monkeys of one of the IgG1 variants indicated that its serum half-life was ~2.5-fold longer than the wild-type Ab. Ag binding was unaffected by the Fc mutations, while several effector functions appeared to be minimally altered. These properties suggest that engineered Abs with longer serum half-lives may prove to be effective therapeutics in humans. ***The Journal of Immunology,*** **2006, 176: 346–356.**

The neonatal FcR (FcRn),[3] a heterodimer comprising β_2-microglobulin (β_2m) and a transmembrane α-chain that is homologous to the α-chain of MHC class I molecules, controls at least two important physiological processes: the passive transfer of maternal IgG to the neonate or fetus and the regulation of serum IgG levels in adults (1). Initial experimental support for its role in IgG homeostasis came from studies in mice deficient in β_2m, and thus lacking functional FcRn, which indicated an unusually short serum half-life for IgG (2–5). A subsequent study with mice deficient in the FcRn α-chain provided further support for this hypothesis (6). The functional expression of FcRn in the vascular endothelium of mice (7) implies that these cells are involved in IgG homeostasis. Recent in vitro studies analyzed the intracellular trafficking of IgG in human endothelial cells (8–11), providing further evidence of a role for these cells in IgG homeostasis.

A hallmark of FcRn is that binding of IgG is exquisitely pH dependent, with IgG binding to FcRn at pH 6.0–6.5 and releasing at pH 7.0–7.5 (12). Consistent with this pH dependence, a model has been proposed (1) to explain how FcRn regulates the serum half-life of IgG. According to the model, serum IgG is initially taken up by fluid-phase pinocytosis into endothelial cells, then IgG binds to FcRn in the more acidic environment of the endosomes, and finally IgG is recycled to the cell surface and returned to the circulation. Thus, FcRn functions as a salvage receptor, rescuing IgG from a lysosomal degradation pathway. Because binding of IgG to FcRn is saturable, it follows that when serum IgG levels rise above the normal level, excess IgG is degraded via the lysosomes. Conversely, if serum IgG levels fall below normal, an increased proportion of serum IgG is salvaged and returned to the circulation.

A correlation has been observed between the FcRn binding affinity of IgG Abs or Fc fragments and their serum half-lives in mice. Variant mouse IgG Fc-hinge fragments with reduced binding affinity for FcRn (13–15) had correspondingly shorter half-lives in mice (15–17). Targeted random mutagenesis of a mouse Fc-hinge fragment led to the generation of mutants with higher binding affinity for mouse FcRn and the identification of a mutant Fc-hinge fragment with increased serum half-life in mice (18).

The correlation between FcRn binding affinity and serum half-life in mice has been extended to human IgG Abs and their fragments. Mutant forms of a human IgG1-derived Fc-hinge fragment with reduced binding to mouse FcRn were found to have shorter half-lives in mice than the wild-type (WT) Fc-hinge fragment (19). In addition, a chimeric mouse-human IgG1 Ab with an amino acid substitution in a key FcRn contact residue was shown to have a shorter half-life in mice compared with the WT chimeric IgG1 Ab (20). Likewise, a humanized IgG1 Ab with no detectable binding to either human or mouse FcRn showed a substantial reduction in its serum half-life in mice (21). Recently, the half-life of a chimeric mouse-human scFv-Fc Ab fragment was fine-tuned by attenuating the Fc·FcRn interaction (22).

Several studies have identified human IgG1 variants with increased binding affinity for human FcRn (23) or for both mouse and human FcRn (24). Although the serum half-lives of the human IgG1 variants were examined in mice (24, 25), no increase in their half-lives was observed. This is presumably because the variants not only showed a significant increase in binding to mouse FcRn at pH 6.0 but also retained substantial binding at pH 7.4.

We recently described the identification of several human IgG2 mutants with increased pH-dependent binding to human FcRn and showed that two of these mutants had serum half-lives in rhesus monkeys that were nearly twice as long as the WT IgG2 Ab (26). In the current study, several mutants of a human IgG1 Ab were generated that showed improved binding to human FcRn at pH 6.0 and demonstrated pH-dependent release. The results of a pharmacokinetics (PK) study in rhesus monkeys with one of the mutant

Protein Design Labs, Fremont, CA 94555

Received for publication August 1, 2005. Accepted for publication October 12, 2005.

The costs of publication of this article were defrayed in part by the payment of page charges. This article must therefore be hereby marked *advertisement* in accordance with 18 U.S.C. Section 1734 solely to indicate this fact.

[1] Address correspondence and reprint requests to Paul R. Hinton, Protein Design Labs, 34801 Campus Drive, Fremont, CA 94555. E-mail address: phinton@pdl.com

[2] Current address: Center for Pharmaceutical Biotechnology, University of Illinois, 900 South Ashland Street, Chicago, IL 60607.

[3] Abbreviations used in this paper: FcRn, neonatal FcR; β_2m, β_2-microglobulin; WT, wild type; PK, pharmacokinetic; HBV, hepatitis B virus; HBsAg, hepatitis B surface antigen; EWB, ELISA wash buffer; RT, room temperature; EB, ELISA buffer; FBB, FACS binding buffer; CDC, complement-dependent cytotoxicity; ADCC, Ab-dependent cell-mediated cytotoxicity.

0022-1767/05/$02.00

IgG1 Abs, as well as the influence of the mutations on Fc-dependent effector functions, are reported.

Materials and Methods

Construction and mutagenesis of IgG expression plasmids

The L and H chain V genes of the human anti-hepatitis B virus (HBV) mAb OST577 (27) were subcloned into plasmids pVλ2 (26) and pVAg1.N, a derivative of pVg1 (28) containing the high copy number bacterial replication origin from pUC18 (29), and an *Nhe*I site in the intron between the hinge and CH2 exons. Expression plasmids were also constructed for production of the IgG1, IgG2M3, and IgG4 forms of Hu1D10 (30), a humanized mAb that recognizes an allele of the HLA-DR β-chain. The plasmid pVk-Hu1D10 was constructed by transferring the Hu1D10 V_L region from pHu1D10.IgG1.rgpt.dE (30) into pVk (28). The plasmids pVAg1.N-Hu1D10 and pVAg2M3-Hu1D10 were constructed by replacing the OST577 V_H region in pVAg1.N-OST577 (this study) and pVAg2M3-OST577 (26), respectively, with the Hu1D10 V_H region from pHu1D10.IgG1.rgpt.dE. The plasmid pHuHCg4.D.Tt-Hu1D10 was constructed by transferring the Hu1D10 V_H region into pHuHCg4.D.Tt, a derivative of pVg2.D.Tt (31) containing the genomic human γ-4 constant region instead of the γ-2 constant region. Overlap-extension PCR (32) was used to generate amino acid substitutions at positions 250 and 428 (numbered according to the EU index (33)) of the IgG1, IgG2M3, and IgG4 H chains.

Expression and purification of IgG Abs

Human kidney cell line 293-H (Invitrogen Life Technologies) was transiently cotransfected with L and H chain plasmids using LipofectAMINE 2000 (Invitrogen Life Technologies) according to the manufacturer's recommendations, and transfected cells were cultured in Hybridoma-SFM serum-free medium (Invitrogen Life Technologies) containing 2% low IgG FBS (HyClone). Mouse myeloma cell line Sp2/0 (American Type Culture Collection) was stably cotransfected by electroporation as described previously (28). The highest Ab-producing clones were adapted and expanded in Hybridoma-SFM serum-free medium or Protein-Free Basal Medium-1 (Protein Design Labs) (34), supplemented after 2 days with Protein-Free Feed Medium-2 (Protein Design Labs) (34), and grown to exhaustion.

Transiently or stably expressed Abs were purified from culture supernatants by protein A column chromatography (Amersham Biosciences). For in vivo studies, the protein A eluate was further purified by size exclusion chromatography using a Superdex 200 column (Amersham Biosciences).

Cloning and cell surface expression of human and rhesus FcRn

Human β_2m and the extracellular domains of the human FcRn α-chain were cloned and expressed in GPI-linked form on the mouse myeloma cell line NS0 (European Collection of Animal Cell Cultures) as previously described (26), yielding cell line NS0-HuFcRn. Similarly, rhesus β_2m and the extracellular domains of the rhesus FcRn α-chain were cloned from rhesus PBMC-derived cDNA and subcloned into pDL172 as previously described (26), yielding pDL410. Cell line NS0 was stably transfected with pDL410 by electroporation, and rhesus FcRn was expressed in GPI-linked form on NS0 cells, yielding cell line NS0-RhFcRn.

Ag binding assays

Binding of WT and mutant OST577-IgG1 Abs to hepatitis B surface Ag (HBsAg) (27) was confirmed in a competitive binding ELISA. Immulon-2 HB 96-well assay plates (Dynex Technologies) were coated with 1 μg/ml HBsAg (Advanced ImmunoChemical) in PBS overnight at 4°C, washed with ELISA wash buffer (EWB) (PBS, 0.1% Tween 20), and blocked with SuperBlock blocking buffer (Pierce) for 30 min at room temperature (RT). The plates were washed with EWB and incubated with biotinylated OST577-IgG1 Ab (0.21 μg/ml) and serial 2-fold dilutions of competitor OST577-IgG1 Abs (80–0.078 μg/ml) in 100 μl of ELISA buffer (EB) (PBS, 1% BSA, 0.1% Tween 20) for 1 h at RT. The plates were washed with EWB, incubated with 1 μg/ml streptavidin-conjugated HRP (Pierce) in EB for 30 min at RT, washed with EWB, and developed by addition of ABTS substrate (Kirkegaard & Perry Laboratories). The reaction was stopped with 2% oxalic acid, and the absorbance at 415 nm was measured using a VERSAmax plate reader (Molecular Devices). IC_{50} values were calculated using GraphPad Prism, version 3.02 (GraphPad).

Binding of WT and mutant Hu1D10-IgG1, IgG2M3, and IgG4 Abs to an allele of the HLA-DR β-chain (30) was confirmed in a competitive FACS binding assay using human Burkitt's lymphoma cell line Raji (American Type Culture Collection), which expresses the Hu1D10 Ag (30). Approximately 2.5×10^5 Raji cells/test were washed with FACS binding buffer (FBB) (PBS, 0.5% BSA, 0.1% NaN_3 (pH 7.4)), and resuspended in biotinylated Hu1D10-IgG1 Ab (4.4 μg/ml) and serial 3-fold dilutions of Hu1D10-IgG1, IgG2M3, or IgG4 competitor Abs (219–0.100 μg/ml) in 160 μl of FBB (pH 7.4). After 1 h on ice, the cells were washed with FBB (pH 7.4) and resuspended in 25 μl of 2.5 μg/ml streptavidin-conjugated PE (BioSource International) in FBB (pH 7.4). After 30 min on ice, the cells were washed with FBB (pH 7.4), resuspended in 1% formaldehyde, and analyzed using a FACSCalibur flow cytometer (BD Immunocytometry Systems). IC_{50} values were calculated using GraphPad Prism.

FcRn binding and pH-dependent release assays

WT and mutant OST577-IgG1 Abs were tested for binding to human or rhesus FcRn in competitive FACS binding assays using serial 3-fold dilutions of competitor OST577-IgG1 Abs (750–0.013 or 500–0.008 μg/ml) essentially as described previously (26). WT and mutant Hu1D10-IgG1, IgG2M3, and IgG4 Abs were tested for binding to human FcRn in a competitive FACS binding assay by modification of the previously described method (26). Briefly, $\sim 2 \times 10^5$ NS0-HuFcRn cells/test were washed as previously described (26) and resuspended in biotinylated human IgG (8.3 μg/ml; Sigma-Aldrich) and serial 3-fold dilutions of competitor Hu1D10-IgG1, IgG2M3, or IgG4 Abs (656–0.011 μg/ml) in 160 μl of FBB (pH 6.0). After 1 h on ice, the cells were processed as previously described (26) and analyzed using a FACSCalibur flow cytometer. IC_{50} values were calculated using GraphPad Prism.

Binding and pH-dependent release of WT and mutant IgG Abs to human or rhesus FcRn was examined in FACS binding assays. Approximately 2×10^5 NS0-HuFcRn or NS0-RhFcRn cells/test were washed with FBB (pH 8.0), then with FBB (pH 6.0), and resuspended in the appropriate IgG Ab (10 μg/ml) in 100 μl of FBB (pH 6.0). After 1 h on ice, the cells were washed with FBB (pH 6.0, 6.5, 7.0, 7.5, or 8.0) and resuspended in 25 μl of 1.25 μg/ml FITC-conjugated goat $F(ab')_2$ anti-human IgG Ab (Southern Biotechnology Associates) or a 1/100 FITC-conjugated goat anti-human κ L chain Ab (Southern Biotechnology Associates), as appropriate, in FBB of the corresponding pH. After 30 min on ice, the cells were washed with FBB of the corresponding pH, resuspended in 1% formaldehyde, and analyzed using a FACSCalibur flow cytometer.

Analysis of rhesus PK study samples

A non-good laboratory practice PK study was approved by the Institutional Animal Care and Use Committee and conducted at the California National Primate Research Center (University of California, Davis). The concentrations of OST577-IgG1 WT and mutant Abs in rhesus serum samples were determined using a validated ELISA. Immulon-2 HB 96-well assay plates were coated with 1 μg/ml mouse anti-OST577 anti-Id mAb (OST577-γ1 anti-id; Protein Design Labs) in PBS overnight at 4°C, washed with EWB, and blocked with SuperBlock blocking buffer for 60 ± 5 min at RT. The plates were washed with EWB, and serum samples (prediluted, if necessary, in pooled normal rhesus serum), calibrators, and positive and negative serum controls that had been appropriately diluted in 100 μl of SuperBlock blocking buffer were incubated for 60 ± 5 min at RT. The plates were washed with EWB and incubated with a 1/1000 dilution of HRP-conjugated goat anti-human λ L chain Ab (Southern Biotechnology Associates) in EB for 60 ± 5 min at RT, washed with EWB, and developed by addition of ABTS substrate for 7 ± 1 min at RT. The reaction was stopped with 2% oxalic acid, and the absorbance at 415 nm was measured within 30 min using a VERSAmax plate reader. The estimated quantitative range of the assay was 0.10–0.90 μg/ml.

The presence of anti-OST577-IgG1 Abs in rhesus serum samples was determined in a bridging ELISA. Maxisorp 96-well assay plates (Nalge Nunc International) were coated with 0.25 μg/ml WT or the T250Q/M428L mutant form of OST577-IgG1 in PBS overnight at 4°C, washed with EWB, and blocked with SuperBlock blocking buffer for 30 min at RT. The plates were washed with EWB, and serum samples (diluted 1/2) or serial 2-fold dilutions of OST577-γ1 anti-id (3.0–0.0015 μg/ml) in 100 μl of EB were incubated for 1 h at RT. The plates were washed with EWB and incubated with biotinylated WT or the T250Q/M428L mutant form of OST577-IgG1 (0.25 μg/ml), respectively, in EB for 1 h at RT. The plates were washed with EWB, incubated with 1 μg/ml streptavidin-conjugated HRP in EB for 30 min at RT, washed with EWB, and developed by addition of ABTS substrate. The plates were processed as described above.

C1q binding assay

Binding of WT and mutant Hu1D10-IgG1, IgG2M3, and IgG4 Abs to human C1q was determined in an ELISA by modification of a previously described method (35). Costar high-binding 96-well assay plates (Corning Life Sciences) were coated with serial 2-fold dilutions of Hu1D10-IgG1,

IgG2M3, or IgG4 Abs (25–0.012 μg/ml) in PBS overnight at 4°C, washed with EWB, and blocked with SuperBlock blocking buffer for 1 h at RT. The plates were washed with EWB, and incubated with 4 μg/ml human C1q (Quidel) in 100 μl of EB for 2 h at RT. The plates were washed with EWB, and incubated with 4 μg/ml biotinylated sheep anti-human C1q (Biodesign International) in EB for 1 h at RT. The plates were washed with EWB, incubated with 3 μg/ml streptavidin-conjugated HRP in EB for 30 min at RT, washed with EWB, and developed by addition of 3,3′,5,5′-tetramethylbenzidine substrate (Kirkegaard & Perry Laboratories). The reaction was stopped with 2 N H_2SO_4, and the absorbance at 450 nm was measured using a VERSAmax plate reader.

Complement-dependent cytotoxicity (CDC)

The CDC activity of WT and mutant Hu1D10-IgG1, IgG2M3, and IgG4 Abs was assayed by modification of a previously described method (30) using human serum as a source of complement and Raji cells as targets. Raji cells were labeled with 50 μCi of ^{51}Cr (Amersham Biosciences) per 10^6 cells in complete medium (RPMI 1640, 10% heat-inactivated FBS), washed, resuspended at a density of 1×10^6 cells/ml in CDC assay medium (RPMI 1640, 10 mM HEPES, 0.1% BSA), and 50 μl/well was added to a Falcon 96-well tissue culture-treated U-bottom assay plate (BD Biosciences). Serial 3-fold dilutions of Hu1D10-IgG1, IgG2M3, or IgG4 Abs (120–0.16 μg/ml) were prepared in CDC assay medium, and 50 μl/well was added to the assay plate. Human serum complement (Quidel) was frozen in aliquots, thawed once for use, diluted 1/4 in CDC assay medium, and 50 μl/well was added to the assay plate. The plates were incubated for 2 h at 37°C in a 7.5% CO_2 incubator. After gentle centrifugation, ^{51}Cr release was measured by counting 75 μl of cell-free supernatant in a Beckman 5500B gamma counter (Beckman Coulter).

Ab-dependent cell-mediated cytotoxicity (ADCC)

The ADCC activity of WT and mutant Hu1D10-IgG1, IgG2M3, and IgG4 Abs was assayed by modification of a previously described method (30) using human PBMC as effectors and Raji cells as targets. Human PBMC were prepared from fresh whole blood using a Ficoll-Paque Plus gradient (Amersham Biosciences) and resuspended at a density of 8×10^6 cells/ml in ADCC assay medium (RPMI 1640, 10% heat inactivated FBS). The FcγRIIIA genotype of donor PBMC was determined as described previously (36). Raji cells were labeled as described above with ^{51}Cr in ADCC assay medium, washed, and resuspended at a density of 0.4×10^6 cells/ml in ADCC assay medium. Serial 3-fold dilutions of Hu1D10-IgG1, IgG2M3, or IgG4 Abs (4.0–0.0055 μg/ml) were prepared in ADCC assay medium. Raji cells (50 μl/well) and Hu1D10 Ab (50 μl/well) were combined in a Corning 96-well tissue culture-treated V-bottom assay plate (Corning Life Sciences) and incubated for 30 min at 4°C to allow opsonization to occur. PBMC (100 μl/well, i.e., 40:1 E:T ratio) were added to the opsonized cells and incubated for 4 h at 37°C in a CO_2 incubator. Ab-independent cell-mediated cytotoxicity was measured by incubating effector and target cells in the absence of Ab. The plates were gently centrifuged, and ^{51}Cr release was measured by counting 100 μl of cell-free supernatant in a Beckman 5500B gamma counter.

Protein A and protein G binding assays

Binding of WT and mutant Hu1D10-IgG1, IgG2M3, and IgG4 Abs to protein A was assayed in a competitive binding ELISA. MaxiSorp 96-well assay plates were coated with 1 μg/ml protein A (Sigma-Aldrich) in PBS overnight at 4°C, washed with EWB, and blocked with SuperBlock blocking buffer for 30 min at RT. The plates were washed with EWB and incubated with biotinylated WT Hu1D10-IgG1, IgG2M3, or IgG4 Abs (0.08 μg/ml) and serial 2-fold dilutions of the appropriate competitor Hu1D10 Ab (333–0.65 μg/ml) in 120 μl/well of EB for 1 h at RT. The plates were washed with EWB, incubated with 1 μg/ml streptavidin-conjugated HRP in EB for 30 min at RT, washed with EWB, and developed by addition of ABTS substrate. Binding of WT and mutant Hu1D10-IgG1, IgG2M3, and IgG4 Abs to protein G was assayed in a competitive binding ELISA essentially as described above, except the plates were coated with 1 μg/ml protein G (Sigma-Aldrich), and 0.25 μg/ml biotinylated WT Hu1D10 Abs was used. IC_{50} values were calculated using GraphPad Prism.

Results

Binding of OST577-IgG1 Abs to FcRn

We previously reported the identification of human IgG2 Fc mutants, namely at positions 250 and 428 (numbered according to the EU index (33)), that have increased binding affinity to human and rhesus FcRn at pH 6.0 and that retained the property of pH-dependent FcRn binding and release. Two of the IgG2 mutants were shown to have serum half-lives in rhesus monkeys ~2-fold longer than the WT Ab (26). One of the IgG2 mutants had a substitution of Met to Leu at Fc position 428 (M428L), and the other mutant had an additional substitution of Thr to Gln at Fc position 250 (T250Q/M428L). Because the amino acids at and around positions 250 and 428 are conserved among all four human IgG subtypes (33), it is of considerable interest to evaluate whether these mutations from the IgG2 subtype would confer a similar FcRn binding phenotype to other IgG subtypes.

Table I. *Binding of OST577 Abs to HBsAg*[a]

OST577	*n*	IC_{50} (μg/ml)	Relative Binding
IgG1 WT	3	0.949 ± 0.059	
IgG1 T250Q	3	1.09 ± 0.07	0.87
IgG1 M428L	3	0.940 ± 0.069	1.0
IgG1 T250Q/M428L	3	1.20 ± 0.13	0.80

[a] Competitive binding experiments were done by ELISA as described in *Materials and Methods.* The mean IC_{50} ± SD are reported for three independent experiments. The relative binding of each mutant was calculated by comparison to the WT.

To examine this hypothesis for an IgG1 subtype Ab, the previously identified T250Q, M428L, and T250Q/M428L mutations were introduced by PCR mutagenesis in the human anti-HBV mAb OST577-IgG1 (27). Binding of the OST577-IgG1 WT and mutant Abs to HBsAg was confirmed in a competitive ELISA (Table I). As expected, the results showed that binding of the T250Q, M428L, and T250Q/M428L IgG1 mutants to HBsAg was nearly identical to that of WT OST577-IgG1, indicating that the Fc mutations had little or no effect on Ag binding.

Binding of the WT and mutant OST577-IgG1 Abs to human FcRn was evaluated in a competitive binding assay at pH 6.0 using a stable transfectant of mouse myeloma cell line NS0 expressing recombinant human FcRn on the cell surface (NS0-HuFcRn). Comparison of the IC_{50} values (Table II) indicated that the single mutants T250Q and M428L showed an increase in binding to human FcRn at pH 6.0 relative to WT IgG1 of ~3- and 11-fold, respectively, while the double mutant T250Q/M428L showed a ~29-fold increase in binding. Similar results were obtained when the WT and mutant Abs were tested for binding to rhesus FcRn. Comparison of the IC_{50} values (Table III) showed that binding of the T250Q, M428L, and T250Q/M428L IgG1 mutants to rhesus FcRn at pH 6.0 was ~3-, 14-, and 37-fold better, respectively, than the WT IgG1 Ab. The relative improvement in binding of the OST577-IgG1 mutants to both human and rhesus FcRn is consistent with the results observed for the corresponding OST577-IgG2 mutants (26).

The interaction of IgG with FcRn is acutely pH dependent, which is consistent with the model of its uptake and release by endothelial cells (1). To confirm that the increased binding of the

Table II. *Binding of OST577 Abs to human FcRn*[a]

OST577	*n*	IC_{50} (μg/ml)	Relative Binding
IgG1 WT	5	10.3 ± 2.8	
IgG1 T250Q	5	3.14 ± 0.86	3.3
IgG1 M428L	5	0.896 ± 0.304	11
IgG1 T250Q/M428L	5	0.351 ± 0.144	29

[a] Competitive binding experiments were done by flow cytometry as described in *Materials and Methods.* The mean IC_{50} ± SD are reported for five independent experiments. The relative improvement in binding for each mutant was calculated by comparison to the WT.

Table III. *Binding of OST577 Abs to rhesus FcRn*[a]

OST577	*n*	IC_{50} (μg/ml)	Relative Binding
IgG1 WT	3	8.86 ± 0.52	
IgG1 T250Q	3	2.97 ± 0.59	3.0
IgG1 M428L	3	0.629 ± 0.060	14
IgG1 T250Q/M428L	3	0.236 ± 0.013	37

[a] Competitive binding experiments were done by flow cytometry as described in *Materials and Methods*. The mean IC_{50} ± SD are reported for three independent experiments. The relative improvement in binding for each mutant was calculated by comparison to the WT.

mutants to FcRn at pH 6.0 did not substantially alter the pH dependence of this interaction, the WT and mutant OST577-IgG1 Abs were allowed to bind to cell line NS0-HuFcRn at pH 6.0 and were then removed by washing the cells at pH 6.0, 6.5, 7.0, 7.5, or 8.0 (Fig. 1*A*). The results for the WT and mutant IgG1 Abs showed that binding to human FcRn was maximal at pH 6.0 and then diminished as the pH of the washes was increased from pH 6.0 to 8.0, with little or no binding observed at pH 7.5 or above. Similar results were obtained when the WT and mutant IgG1 Abs were tested for pH-dependent binding to rhesus FcRn (Fig. 1*B*). The pH-dependent binding results for the IgG1 mutants are similar to those observed for the corresponding IgG2 mutants of OST577 (26). These results affirm that an improved FcRn binding phenotype can be bestowed to the IgG1 subtype by transferring the T250Q, M428L, or T250Q/M428L mutations into the Fc region of a human IgG1 Ab.

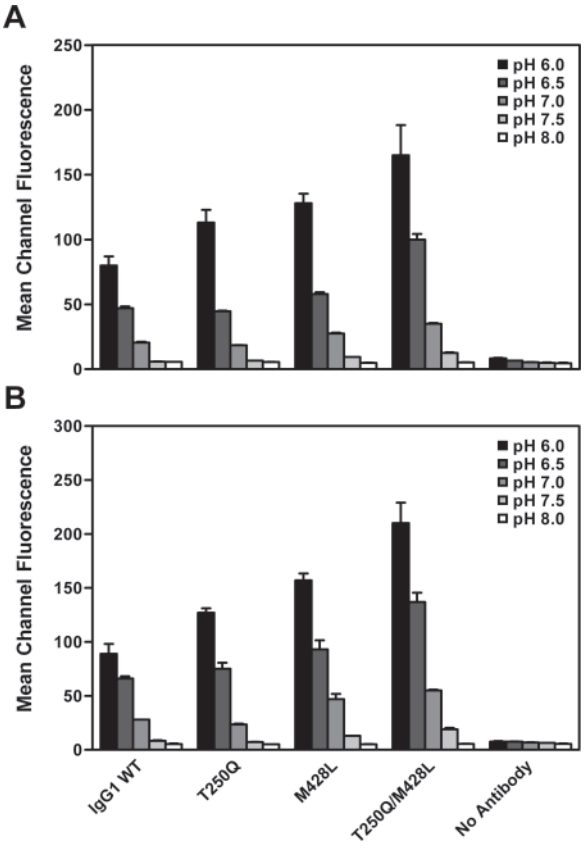

FIGURE 1. Binding and pH-dependent release of OST577-IgG1 WT and mutant Abs to human (*A*) or rhesus (*B*) FcRn. OST577-IgG1 WT or mutant Abs were allowed to bind at pH 6.0 to human or rhesus FcRn expressed on the surface of NS0 cells and washed at the indicated pH values as described in *Materials and Methods*. Bound OST577-IgG1 Abs were detected with FITC-conjugated goat $F(ab')_2$ anti-human IgG Ab and analyzed by flow cytometry. The averaged mean channel fluorescence ± SD from two independent experiments are shown.

PK of OST577-IgG1 Abs in rhesus monkeys

To investigate whether increased pH-dependent binding to FcRn correlates with longer serum half-life, the PK behavior of the OST577-IgG1 WT and T250Q/M428L mutant Abs was evaluated in rhesus monkeys. Eight male rhesus macaques, which had been screened and determined to be HBsAg negative, were randomized by weight and assigned to one of two study groups. Each animal received a single i.v. dose of WT or the T250Q/M428L mutant form of OST577-IgG1 at 1 mg/kg by infusion over a span of 15 min. Blood samples were drawn before dosing on day 0, at 1 and 4 h after dosing, and at 1, 7, 14, 21, 28, 42, and 56 days. The concentrations of the OST577-IgG1 WT and mutant Abs in rhesus serum samples were determined using a validated ELISA as described in *Materials and Methods*.

The results of the PK study indicated that the mean serum Ab concentration of the T250Q/M428L mutant was maintained at higher levels than WT OST577-IgG1 at all time points throughout the study (Fig. 2). The mean maximum serum Ab concentration (C_{max}) values were similar between the two test groups (Table IV), suggesting that the administered Abs were distributed to the circulation in a similar manner. Thus, the higher concentration of the T250Q/M428L mutant is attributable to its increased persistence in the serum, rather than altered distribution to the systemic circulation. The mean clearance (CL) was ~2.3-fold lower for the T250Q/M428L mutant (0.0811 ± 0.0191 ml/h/kg; $p = 0.029$) compared with WT OST577-IgG1 (0.190 ± 0.022 ml/h/kg) (Table IV), indicating a significant decrease in the clearance of the OST577-IgG1 T250Q/M428L mutant. The area under the concentration-time curve (AUC) was ~2.4-fold higher for the T250Q/M428L mutant (12,900 ± 3,000 h·μg/ml; $p = 0.029$) compared with WT OST577-IgG1 (5,320 ± 590 h·μg/ml) (Table IV), indicating a significant increase in the total exposure of the OST577-IgG1 T250Q/M428L mutant. Finally, the elimination (β-phase) half-life ($t_{1/2}$) was ~2.5-fold longer for the T250Q/M428L mutant

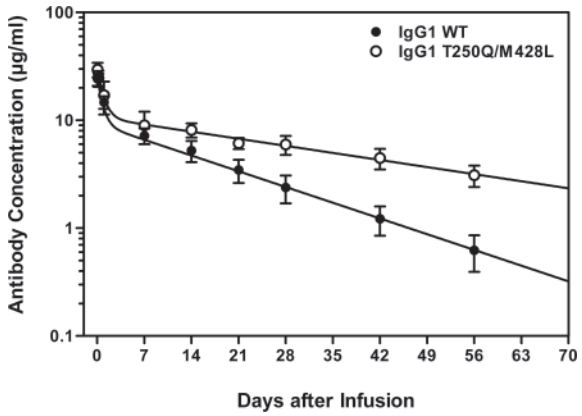

FIGURE 2. PK profile of OST577-IgG1 WT and mutant Abs in rhesus monkeys. The concentration of OST577-IgG1 Abs in rhesus sera was measured in a validated ELISA using mouse anti-OST577 anti-Id mAb for capture and HRP-conjugated goat anti-human λ L chain Ab for detection. The serum Ab concentration data were fitted with a two-compartment model using WinNonlin Enterprise Edition, version 3.2 (Pharsight). Mann-Whitney tests were done using GraphPad Prism, version 3.02. The modeled data (simulated based on the mean values of each group's primary PK parameters), as well as the observed mean serum Ab concentration (μg/ml) ± SD for each group of four animals, were plotted as a function of time (days after infusion).

Table IV. *Summary of PK parameters*[a]

OST577	C_{max}[b] (μg/ml)	CL (ml/h/kg)	AUC (h·μg/ml)	$t_{1/2}$ (h)
IgG1 WT	26.0 ± 4.1	0.190 ± 0.022	5,320 ± 590	336 ± 34
IgG1 T250Q/M428L	29.1 ± 3.7	0.0811* ± 0.0191	12,900* ± 3,000	838* ± 187

[a] The group mean ± SD are reported for each parameter. *, indicates a significant difference ($p < 0.05$) between the WT and mutant groups.
[b] C_{max}, maximum serum Ab concentration; CL, clearance; AUC, area under the concentration-time curve; $t_{1/2}$, elimination (β-phase) half-life.

(838 ± 187 h; $p = 0.029$) compared with WT OST577-IgG1 (336 ± 34 h) (Table IV), indicating a significant increase in the serum half-life of the OST577-IgG1 T250Q/M428L mutant. The elimination half-life for WT OST577-IgG1 in this study is indistinguishable from that observed for OST577-IgG1 (324 ± 85 h) in a previous PK study in rhesus monkeys (27).

There was no indication of immunogenicity from the PK behavior of the OST577-IgG1 WT and T250Q/M428L mutant Abs in rhesus monkeys. Inspection of the serum Ab concentrations in the eight individual animals showed that there was a steady decline in the Ab levels from days 7 through 56 (data not shown), with no trend toward an accelerated decline that might be indicative of a rhesus anti-human Ab response. Moreover, when the rhesus serum samples from days 0 (predose), 7, 21, and 56 were analyzed for anti-Ab activity in a bridging ELISA as described in *Materials and Methods*, none of the eight animals tested positive (data not shown), suggesting that neither the OST577-IgG1 WT nor the T250Q/M428L mutant was immunogenic in rhesus monkeys.

Binding of Hu1D10 Abs to FcRn

To determine whether the enhanced FcRn binding phenotype conferred by the T250Q/M428L mutation could be transferred to an Ab with a different Ag-binding specificity and L chain type, a panel of human IgG1, IgG2M3, and IgG4 WT and T250Q/M428L mutant forms of the humanized anti-HLA-DR β-chain allele mAb Hu1D10 (30) was constructed. Hu1D10 was chosen because the IgG1 form of this Ab demonstrates both CDC and ADCC activities (30), enabling the comparison of important effector functions between the mutants and the corresponding WT Abs. IgG2M3 is a variant of IgG2 that has been engineered to minimize binding to FcγR (31). The IgG3 form was excluded from the panel because this subtype is seldom considered for therapeutic applications.

Binding of the Hu1D10-IgG1, IgG2M3, and IgG4 WT and T250Q/M428L mutant Abs to the HLA-DR β-chain allele was assessed by flow cytometry in a competitive binding assay (Table V). Binding of each of the T250Q/M428L mutants to Raji cells was very similar to that of the corresponding WT Hu1D10 Ab, confirming that the Fc mutations had little effect on Ag binding. A slight reduction in the binding avidity of the IgG2M3 and IgG4 forms was observed compared with the IgG1 forms of the Hu1D10 Ab (Table V). Previous studies have also documented decreased avidity of the IgG2 (31, 37) and IgG4 (37) subtypes relative to the IgG1 subtype, which is consistent with the results of this study.

Binding of the WT and T250Q/M428L mutant forms of the Hu1D10-IgG1, IgG2M3, and IgG4 Abs to human FcRn was evaluated in a competitive binding assay. The Abs were competed against pooled human serum IgG to more closely simulate in vivo conditions. Comparison of the IC_{50} values (Table VI) indicated that the T250Q/M428L forms of the Hu1D10-IgG1, IgG2M3, and IgG4 Abs showed a substantial increase in binding to human FcRn at pH 6.0 compared with the corresponding WT Hu1D10 Abs. Similar results were observed when the experiments were repeated using transiently expressed WT and double mutant forms of the Hu1D10-IgG1, IgG2M3, and IgG4 Abs (data not shown). Slight differences in binding to human FcRn were observed among the WT human IgG subtypes (Table VI), as noted in an earlier study (38), although the rank order among the IgG subtypes in this study differs from that in the previous study. A substantial improvement in binding was also observed when the T250Q/M428L mutant forms of the Hu1D10-IgG1, IgG2M3, and IgG4 Abs were compared with the corresponding WT Abs for binding to rhesus FcRn at pH 6.0 (data not shown).

To confirm that binding to FcRn was pH dependent, the Hu1D10-IgG1, IgG2M3, and IgG4 WT and T250Q/M428L mutant Abs were tested for binding and pH-dependent release using NS0-HuFcRn cells (Fig. 3). The results showed that binding of the WT and T250Q/M428L mutant Hu1D10 Abs to human FcRn was maximal at pH 6.0, with little or no binding observed at pH 7.5 or above. Similar results were obtained when the WT and T250Q/M428L mutant Hu1D10 Abs were tested for pH-dependent binding to rhesus FcRn (data not shown), suggesting that pH-dependent binding to both human and rhesus FcRn was retained in the IgG1, IgG2M3, and IgG4 mutants. These data support the conclusions that the enhanced FcRn binding phenotype conferred by the T250Q/M428L mutation can be transferred to an Ab with a different Ag-binding specificity and L chain type and that the double mutation imparts a similar relative increase in binding to both human and rhesus FcRn among the human IgG1, IgG2M3, and IgG4 subtypes.

Table V. *Binding of Hu1D10 Abs to Raji cells*[a]

Hu1D10	*n*	IC_{50} (μg/ml)	Relative Binding
IgG1 WT	3	2.44 ± 0.22	
IgG1 T250Q/M428L	3	2.46 ± 0.35	1.0
IgG2M3 WT	3	4.11 ± 0.56	
IgG2M3 T250Q/M428L	3	3.81 ± 0.49	1.1
IgG4 WT	3	4.89 ± 0.63	
IgG4 T250Q/M428L	3	3.46 ± 0.46	1.4

[a] Competitive binding experiments were done by flow cytometry as described in *Materials and Methods.* The mean IC_{50} ± SD are reported for three independent experiments. The relative binding of each mutant was calculated by comparison to the corresponding WT.

Table VI. *Binding of Hu1D10 Abs to human FcRn*[a]

Hu1D10	*n*	IC_{50} (μg/ml)	Relative Binding
IgG1 WT	5	8.98 ± 1.21	
IgG1 T250Q/M428L	5	0.305 ± 0.114	29
IgG2M3 WT	5	32.2 ± 6.6	
IgG2M3 T250Q/M428L	5	1.27 ± 0.64	25
IgG4 WT	5	27.3 ± 2.5	
IgG4 T250Q/M428L	5	0.558 ± 0.100	49

[a] Competitive binding experiments were done by flow cytometry as described in *Materials and Methods.* The mean IC_{50} ± SD are reported for five independent experiments. The relative improvement in binding for each mutant was calculated by comparison to the corresponding WT.

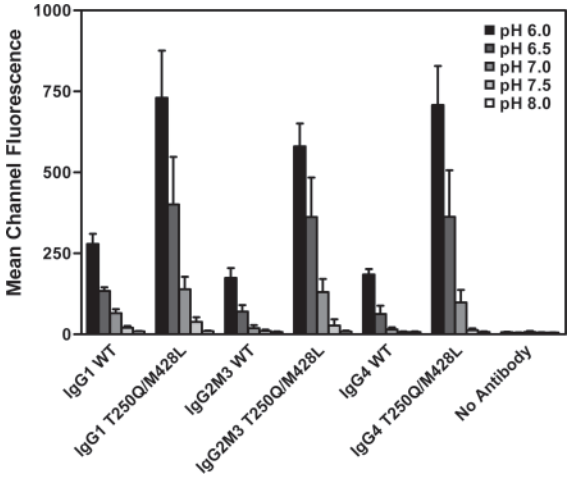

FIGURE 3. Binding and pH-dependent release of Hu1D10 WT and mutant Abs to human FcRn. Hu1D10-IgG1, IgG2M3, and IgG4 WT or mutant Abs were allowed to bind at pH 6.0 to human FcRn expressed on the surface of NS0 cells and washed at the indicated pH values as described in *Materials and Methods*. Bound Hu1D10 Abs were detected with FITC-conjugated goat anti-human κ L chain Ab and analyzed by flow cytometry. The averaged mean channel fluorescence ± SD from three independent experiments are shown.

C1q binding and CDC activity of Hu1D10 Abs

CDC is one of the effector functions by which IgG1 Abs mediate lysis of target cells. Complement activation is initiated by binding of C1q to the Fc region of IgG or IgM Abs complexed with Ag. To examine whether the T250Q/M428L mutation affected CDC, binding of the WT and T250Q/M428L mutant forms of the Hu1D10-IgG1, IgG2M3, and IgG4 Abs to human C1q was determined in an ELISA (Fig. 4). The Hu1D10-IgG1 WT and T250Q/M428L mutant Abs showed strong binding activity, and their binding patterns were indistinguishable from each other in this assay, indicating that C1q binding of the IgG1 subtype was not affected by the mutations, whereas the WT and T250Q/M428L mutant forms of the Hu1D10-IgG2M3 and IgG4 Abs showed lower binding activity. Similar results were obtained when the Abs were transiently expressed (data not shown). The relative C1q binding activities of the WT Hu1D10-IgG1, IgG2M3, and IgG4 Abs in this study are consistent with the C1q binding activities reported for these IgG subtypes in previous studies (35, 39–43).

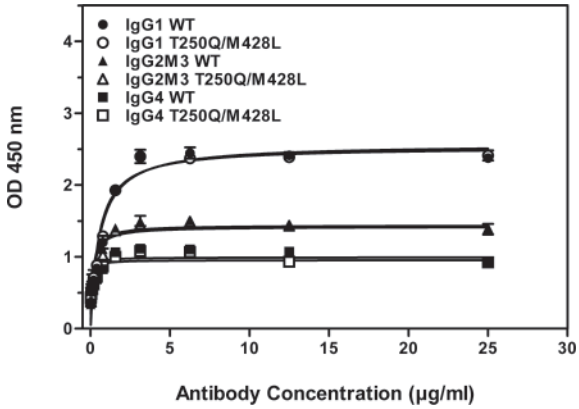

FIGURE 4. Binding of Hu1D10 WT and mutant Abs to human C1q. Binding of Hu1D10-IgG1, IgG2M3, and IgG4 WT or mutant Abs to human C1q was measured by ELISA as described in *Materials and Methods*. The relative binding efficiency of each Ab to the assay plate was found to be similar using HRP-conjugated goat anti-human κ L chain Ab (data not shown). The mean ± SD of replicate samples are shown. The data are representative of three independent experiments.

The CDC activity of the Hu1D10-IgG1, IgG2M3, and IgG4 WT and T250Q/M428L mutant Abs was assayed using human serum as a source of complement and Raji cells as targets (Fig. 5*A*). The Hu1D10-IgG1 WT Ab showed significant CDC activity in this assay, as reported previously (30). Interestingly, the Hu1D10-IgG1 T250Q/M428L mutant Ab showed ~2-fold higher potency (EC_{50}) in this assay than WT Hu1D10-IgG1 and a slight increase in efficacy (maximal percent activity), despite showing no change in its C1q binding activity. A somewhat greater difference in potency was observed between the T250Q/M428L and WT forms of Hu1D10-IgG1 when different preparations of the Abs were compared (data not shown). As expected, the WT and T250Q/M428L mutant forms of the Hu1D10-IgG2M3 and IgG4 Abs did not show significant CDC activity. When the experiment was repeated using transiently expressed Abs (Fig. 5*B*), the Hu1D10-IgG1 WT and T250Q/M428L mutant Abs showed no difference in potency, whereas the Hu1D10-IgG2M3 and IgG4 Abs did not show significant CDC activity.

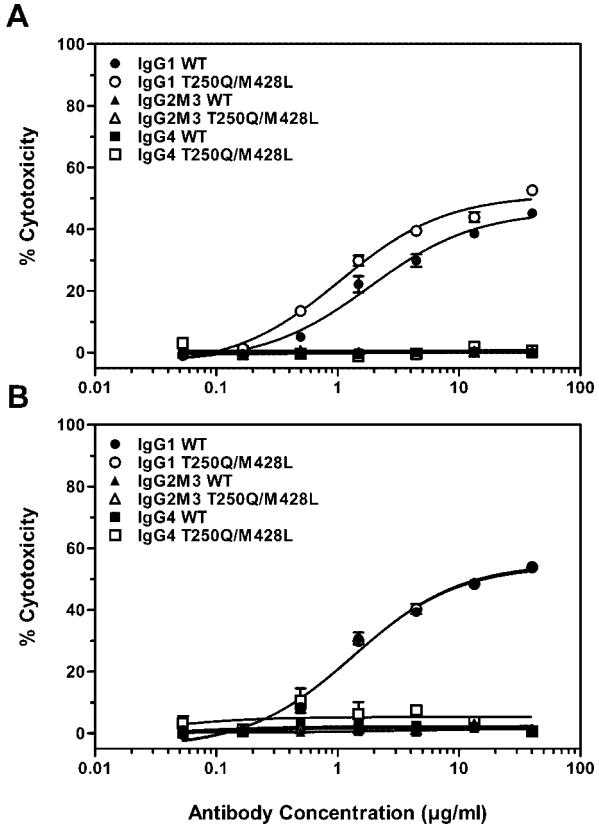

FIGURE 5. CDC activity of Hu1D10 WT and mutant Abs using human complement. The CDC activity of stably (*A*) or transiently (*B*) expressed Hu1D10-IgG1, IgG2M3, and IgG4 WT or mutant Abs at various concentrations was analyzed using a ^{51}Cr release assay as described in *Materials and Methods*. Human serum diluted 1/12 was used as a source of complement and Raji cells were used as targets. Spontaneous release ($cpm_{spontaneous}$) was measured by incubating target cells in the absence of Ab. Maximum release ($cpm_{maximum}$) was measured by adding Triton X-100 to 1% to target cells. The percent lysis was calculated as: percentage of cytotoxicity = $((cpm_{sample} - cpm_{spontaneous})/(cpm_{maximum} - cpm_{spontaneous})) \times 100$. The mean ± SD of replicate samples are shown. The data are representative of six (*A*) or five (*B*) independent experiments.

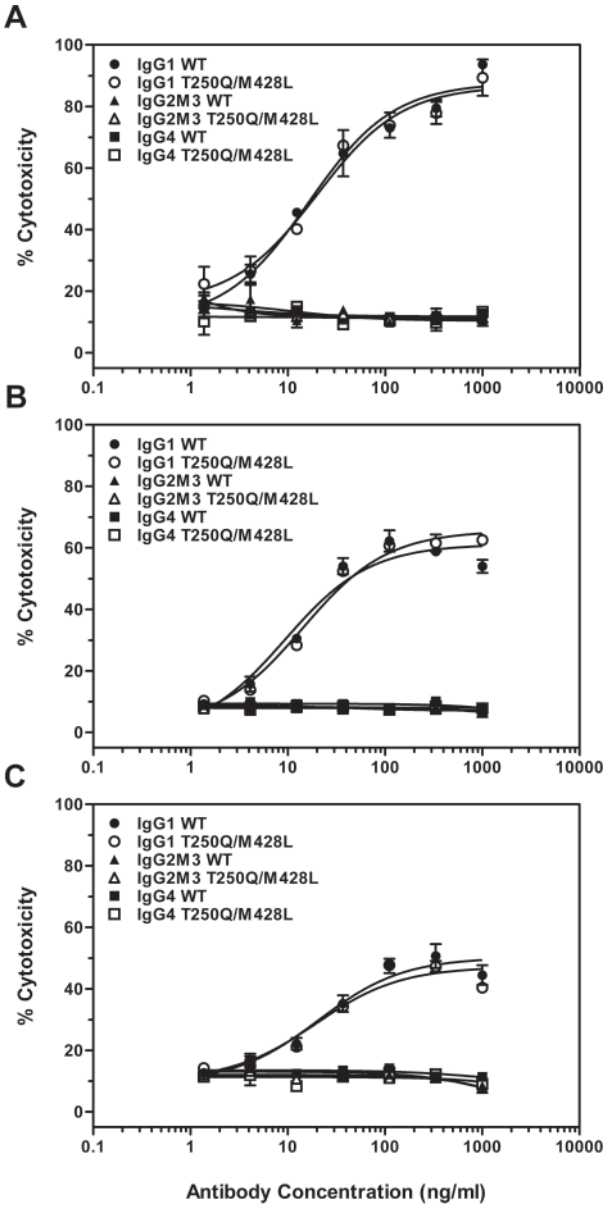

FIGURE 6. ADCC activity of Hu1D10 Abs using PBMC from 158V/V (*A*), 158V/F (*B*), or 158F/F (*C*) donors. The ADCC activity of Hu1D10-IgG1, IgG2M3, and IgG4 WT or mutant Abs at various concentrations was measured using a ^{51}Cr release assay as described in *Materials and Methods*. Human PBMC were used as effectors and Raji cells were used as targets at an E:T ratio of 40:1. Spontaneous release ($cpm_{spontaneous}$) was measured by incubating target cells in the absence of Ab. Maximum release ($cpm_{maximum}$) was measured by adding Triton X-100 to 1% to target cells. The percent lysis was calculated as: percentage of cytotoxicity = $((cpm_{sample} - cpm_{spontaneous})/(cpm_{maximum} - cpm_{spontaneous})) \times 100$. The mean ± SD of replicate samples are shown. The data are representative of five (*A*), six (*B*), or six (*C*) independent experiments.

ADCC activity of Hu1D10 Abs

ADCC is another important effector mechanism leading to the destruction of target cells by IgG Abs. This process is mediated through the engagement of various FcγRs on effector cells, particularly FcγRIIIA on NK cells, by the Fc region of IgG Abs on opsonized target cells. The ADCC activity of the WT and T250Q/M428L mutant forms of the Hu1D10 IgG1, IgG2M3, and IgG4 Abs was assayed using human PBMC as effectors and Raji cells as targets (Fig. 6). Because an allelic polymorphism at amino acid position 158 of FcγRIIIA has been shown to impact both the binding of human IgG1 Abs to NK cells (36, 44) as well as their ADCC activity (23, 45), PBMC from 158V/V, 158V/F, or 158F/F donors were used. When PBMC from a 158V/V donor were used, the Hu1D10-IgG1 T250Q/M428L mutant Ab showed similar potency in this assay compared with WT Hu1D10-IgG1 (Fig. 6*A*). Similar results were observed using PBMC from 158V/F (Fig. 6*B*) or 158F/F (Fig. 6*C*) donors. Moderate differences in potency were observed when different preparations of the Hu1D10-IgG1 WT and T250Q/M428L Abs were compared using PBMC from 158V/V, 158V/F, or 158F/F donors (data not shown). When the experiments were repeated using transiently expressed Abs, no differences were observed in the potency of the Hu1D10-IgG1 T250Q/M428L mutant compared with the Hu1D10-IgG1 WT Ab using PBMC from donors of all three genotypes (data not shown). The efficacy of the Hu1D10-IgG1 WT and T250Q/M428L mutant Abs appeared similar to each other for any given donor (Fig. 6) but varied between donors. Similar results were obtained with additional donors of each genotype (data not shown). The variation in efficacy among donors was presumably due to either FcγRIIIA genotype differences (36, 44) or donor-specific differences in the relative abundance of NK cells in their PBMC (46). As expected, the Hu1D10-IgG2M3 and IgG4 WT and T250Q/M428L mutant Abs did not show significant ADCC activity using PBMC from 158V/V, 158V/F, or 158F/F donors (Fig. 6).

Binding of Hu1D10 Abs to protein A and protein G

Protein A and protein G bind to a region at the CH2-CH3 domain interface that overlaps the FcRn binding site (47). Thus, Fc mutations that alter binding to FcRn might also be expected to affect binding to either protein A or protein G. Because these proteins are often used for purification of IgG Abs, it is of practical importance to determine whether the mutations at positions 250 and 428 affected binding to protein A or protein G.

Binding of WT and mutant Hu1D10-IgG1, IgG2M3, and IgG4 Abs to protein A (Table VII) or protein G (Table VIII) was assayed in competitive binding ELISA experiments. The results showed that binding of the T250Q/M428L mutant forms of the Hu1D10-IgG1, IgG2M3, and IgG4 Abs to protein A was reduced ~2- to 3-fold compared with the corresponding WT forms of this Ab (Table VII). Similar results were seen for the WT and mutant OST577-IgG1 Abs when compared in competitive ELISA experiments for binding to protein A (data not shown). Despite this, each of the T250Q/M428L mutant Abs could be purified by protein A chromatography, and yields of the WT and mutant Hu1D10 or OST577 Abs were comparable (data not shown). Binding of the WT and T250Q/M428L mutant forms of the Hu1D10-IgG1, IgG2M3, and IgG4 Abs to protein G was comparable (Table VIII). Similarly, no differences were seen for the WT and mutant

Table VII. *Binding of Hu1D10 Abs to protein A*[a]

Hu1D10	*n*	IC_{50} (μg/ml)	Relative Binding
IgG1 WT	5	20.4 ± 5.5	
IgG1 T250Q/M428L	5	61.5 ± 35.3	0.33
IgG2M3 WT	3	8.32 ± 0.83	
IgG2M3 T250Q/M428L	3	27.2 ± 2.7	0.31
IgG4 WT	3	25.0 ± 3.6	
IgG4 T250Q/M428L	3	58.9 ± 5.3	0.42

[a] Competitive binding experiments were done by ELISA as described in *Materials and Methods*. The mean IC_{50} ± SD are reported for three to five independent experiments. The relative improvement in binding for each mutant was calculated by comparison to the corresponding WT.

Table VIII. *Binding of Hu1D10 Abs to protein G*[a]

Hu1D10	*n*	IC_{50} (μg/ml)	Relative Binding
IgG1 WT	3	14.3 ± 2.5	
IgG1 T250Q/M428L	3	16.5 ± 4.5	0.87
IgG2M3 WT	3	11.7 ± 1.2	
IgG2M3 T250Q/M428L	3	16.3 ± 2.2	0.72
IgG4 WT	3	19.6 ± 1.0	
IgG4 T250Q/M428L	3	21.5 ± 7.7	0.91

[a] Competitive binding experiments were done by ELISA as described in *Materials and Methods.* The mean IC_{50} ± SD are reported for three independent experiments. The relative improvement in binding for each mutant was calculated by comparison to the corresponding WT.

OST577-IgG1 Abs when compared in competitive ELISA experiments for binding to protein G (data not shown).

Discussion

With the aim of improving binding of human IgG to human FcRn at pH 6.0, positions 250 and 428 of the human IgG Fc were chosen, with the aid of computer modeling, for mutagenesis. We previously described several human IgG2 mutants with substitutions at these positions that showed increased pH-dependent binding to human FcRn (26). The mutations T250Q and M428L were found to have an additive effect when combined, resulting in a T250Q/M428L double mutant with an even more substantial improvement in FcRn binding. The effect of the T250Q/M428L double mutation on Ab serum half-life was previously examined using a human IgG2 Ab (OST577-IgG2M3) with specificity to the surface Ag of HBV. A rhesus PK study (26) indicated that the terminal elimination half-life of the OST577-IgG2M3 T250Q/M428L variant (~27 days) was increased ~2-fold compared with that of the OST577-IgG2M3 WT control Ab (~15 days). Because the amino acids at and around positions 250 and 428 in the Fc region are conserved among the four human IgG subtypes (33), it is of significant interest to investigate whether a similar phenotype would occur by transferring mutations that resulted in improved FcRn binding from the human IgG2 subtype to other human IgG subtypes. In concordance with the results reported for the IgG2M3 form of OST577 (26), the results of this study indicate that the mutations T250Q, M428L, and T250Q/M428L conferred similar improvements in relative binding of the IgG1 subtype to both human and rhesus FcRn at pH 6.0 and that binding to human and rhesus FcRn was pH dependent. A rhesus PK study showed that the OST577-IgG1 T250Q/M428L variant had a ~2.5-fold longer terminal elimination half-life (~35 days) when compared with that of the OST577-IgG1 WT control Ab (~14 days).

The role of glycosylation of the CH2 domain in modulating the serum half-lives of IgG Abs remains controversial. Several observations suggest glycosylation makes a negligible contribution to the serum half-life of IgG Abs. First, binding of human IgG1 to human FcRn was unaffected in a genetically aglycosylated IgG1 variant (23) and in a full-length IgG1 produced in *Escherichia coli* (48). Second, the serum half-lives of recombinant human IgG1 Abs were similar for aglycosylated and WT Abs in mice (49–53), cynomolgus monkeys (53), rhesus monkeys (51, 53), and chimpanzees (48). Third, comparison of chimeric human IgG1 Abs differing in their carbohydrate structures (54) showed that Abs lacking terminal sialic acid or galactose residues had serum half-lives in mice that were identical to WT Abs (55). However, aglycosylated human IgG3 Abs were cleared more rapidly than WT IgG3 Abs in mice (49). Analysis of the carbohydrates attached to the OST577-IgG1 WT and T250Q/M428L mutant Abs used for the rhesus PK study revealed that both Abs consisted primarily of the G0, G1, and G2 glycoforms (data not shown). Thus, it seems unlikely that differences in glycosylation significantly contributed to the longer serum half-life of the OST577-IgG1 T250Q/M428L mutant Ab, although it is possible that minor glycosylation differences may subtly modulate the PK profiles of the Abs.

Mutagenesis studies (21, 23, 24) have identified several human IgG1 Fc residues that appear to be critically important in mediating binding to human FcRn at pH 6.0, including I253, S254, H435, and Y436, because replacement of these residues with Ala substantially reduced binding. A model of the interaction between human FcRn and the human IgG1 Fc, based on the crystal structure of a complex between rat FcRn and a rat IgG2a Fc heterodimer (56), was used to predict that all four of these human Fc residues are likely to contact human FcRn. Additional human IgG1 Fc residues predicted to contact human FcRn (56), including K288, L309, and H433, showed a more moderate reduction in binding to FcRn when mutated to Ala (23). Several predicted noncontact residues (56), such as R255 and S415, also showed a moderate reduction in FcRn binding following Ala replacement (23).

Previous mutagenesis studies (23, 24) have also identified human IgG1 Fc mutants that demonstrated improved binding to human FcRn at pH 6.0. Individual Fc substitutions that resulted in at least a 2-fold improvement in FcRn binding include M252W, M252Y, E380A, and N434A; further improvements in binding were observed when multiple substitutions were made (23, 24). However, no functional improvement in the serum half-lives of the resulting Abs was observed in mice (24, 25) or reported in primates.

Analyses of the crystal structures of the human IgG1 Fc region (57, 58) as well as inspection of models of the human IgG Fc·FcRn complex (Fig. 7) indicated that amino acid residues 250 and 428 of the human IgG Fc appear to be buried near the CH2-CH3 interface but are not predicted to contact human FcRn (56). Thus, we hypothesize that mutations at these positions increase the affinity of the human Fc for human FcRn by affecting the conformation of

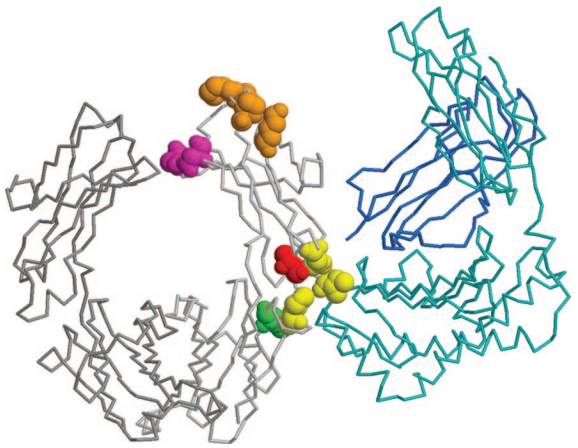

FIGURE 7. Molecular model of human IgG Fc·FcRn complex. The Fc chains are light gray (proximal to FcRn) and dark gray (distal to FcRn); for the receptor, β_2m is dark blue, and the FcRn α-chain is light blue. Residue T250 is shown in red and M428 is in green. Shown in yellow are residues (I253, H310, H435) that are critically important for pH-dependent binding to FcRn (1). Depicted in orange are residues (D270, K322, P329, P331) comprising the core binding site for C1q (35). Indicated in magenta are several residues (D265, N297) critical for FcγR binding (23); additional residues important for FcγR binding are not represented in the model. The model was built from the experimental structure of the rat Fc·FcRn complex (56).

neighboring residues comprising the FcRn binding site, resulting in IgG Abs with longer serum half-lives. Alternatively, it is possible that mutations at these positions may have different mechanisms of modulating the interaction of IgG with human FcRn. The T250Q, M428L, and T250Q/M428L mutations conferred improved pH-dependent binding to human and rhesus FcRn to both the IgG1 (this study) and IgG2 (26) forms of OST577 (27), a human Ab that binds HBsAg. When the T250Q/M428L double mutation was transferred to the IgG1, IgG2, and IgG4 forms of Hu1D10, a humanized Ab that binds to an allele of the β-chain of HLA-DR molecules (30), a similar improvement in relative binding to human and rhesus FcRn at pH 6.0 was observed for the T250Q/M428L mutant compared with the WT form for each IgG subtype of the Hu1D10 Ab. These results suggest that the mutations at positions 250 and 428 have a similar effect on the conformation of the FcRn binding site among these three IgG subtypes. In addition, V region sequences do not appear to influence the effect of the T250Q/M428L mutation on binding to FcRn. Moreover, because the OST577 Abs have λ L chains (27) while the Hu1D10 Abs have κ L chains (30), it appears that the effects of these H chain mutations on binding to FcRn are independent of the L chain type. Taken together, it may be concluded that the T250Q/M428L double mutation can increase the terminal elimination half-life of any IgG1, IgG2, or IgG4 Ab.

Binding of C1q, the first component of the classical complement pathway, to IgG or IgM complexed with Ag initiates activation of the complement cascade. Previous mutagenesis studies localized the C1q binding site to a region in the upper CH2 domain of human IgG1 (35, 39, 40, 43, 59) that does not appear to overlap the FcRn binding site (Fig. 7). Mutations in the lower hinge region of human IgG1 were also found to play a role in modulating C1q binding and CDC activity (41–43). Hence, Fc mutations altering the human FcRn binding site might be expected to have minimal impact on C1q binding or CDC activity. However, several studies (35, 43) identified human IgG1 mutants with altered C1q binding and CDC activity that retained normal (35) or slightly reduced (43) binding to human FcRn. Thus, it was of interest to determine whether mutations at positions 250 or 428, which led to improved binding to FcRn, might alter C1q binding or CDC activity.

The T250Q/M428L double mutation had no effect on binding of C1q to the Hu1D10-IgG1 Abs. Nonetheless, the stably expressed Hu1D10-IgG1 T250Q/M428L variant exhibited moderately increased CDC activity compared with the WT control Ab, while no difference was observed between the IgG1 forms when the Abs were transiently expressed. It is possible that the C1q binding assay was not sensitive enough to detect a small difference in binding between the WT and T250Q/M428L mutant Abs. Alternatively, the T250Q or M428L mutations, or their combination, might be affecting a step in the cascade of complement activation other than C1q binding. However, because the CDC activity of the WT and T250Q/M428L mutant forms of Hu1D10-IgG1 varied slightly when the Abs were expressed in different mammalian host cells, it is conceivable that differences in cell type or culture conditions might result in altered posttranslational modifications (e.g., glycosylation) that could influence CDC activity. This interpretation is consistent with several studies indicating that glycosylation differences in the Fc region of human IgG1 Abs may affect CDC activity (60, 61). Hence, the T250Q/M428L mutation per se may have very little impact, if any, on CDC activity.

ADCC is another important Fc-mediated effector mechanism resulting in target cell lysis by IgG Abs. Binding of IgG to FcγRIIIA on NK cells is believed to play a key role in this process. Several genetic polymorphisms have been described for FcγRIIIA, including a V/F polymorphism at position 158 (36, 44). These studies further indicated that NK cells from FcγRIIIA-158V homozygous donors (158V/V) showed stronger binding to human IgG1 than NK cells from FcγRIIIA-158F homozygous donors (158F/F) (36, 44). Indeed, the 158V/V genotype has been shown to have higher ADCC activity (23, 45), and in some studies, the FcγRIIIA genotype was associated with the clinical response to therapeutic Abs (62–65).

Previous mutagenesis studies have implicated the lower hinge region of human IgG1 in binding to human FcγRIIIA (23, 41, 43). Recently, comprehensive alanine scanning mutagenesis was used to map the binding site on human IgG1 for various human FcγRs (23), including FcγRIIIA. Residues affecting FcγRIIIA binding generally clustered at the hinge-proximal end of the CH2 domain (Fig. 7), including the lower hinge region, and had no effect on FcRn binding (23). However, several residues near the CH2-CH3 interface were also identified, notably T256 and D376, that had a modest effect on binding to both FcRn and FcγRIIIA when substituted with Ala (23). Thus, it was of interest to investigate whether mutations at positions 250 and 428 resulting in improved FcRn binding might alter ADCC activity. The Hu1D10-IgG1 T250Q/M428L variant was shown to have ADCC activity comparable to the WT control Ab, suggesting that the T250Q/M428L mutation has little or no effect on ADCC activity.

It has been proposed that a set of core residues in the Fc forms a consensus binding site that is common to various proteins known to bind at the CH2-CH3 interface (e.g., FcRn, protein G, protein A, and rheumatoid factor), with additional contacts formed by adjacent residues (47). This shared set of contact residues comprises Fc residues M252, I253, S254, N434, H435, and Y436, with additional contacts in some of the complexes formed by residues E380, R255, and H433. Based on the crystal structure of the complex of the C2 domain of streptococcal protein G and the Fc fragment of human IgG1 (66), Fc residue M428 is predicted to participate in a hydrophobic interaction upon complex formation with protein G, whereas Fc residue T250 is not predicted to contribute to this interaction. Neither Fc residue T250 nor residue M428 is predicted to participate in the interaction between fragment B of protein A and the human IgG1 Fc based on the crystal structure of this complex (57). Thus, it is somewhat surprising that the T250Q/M428L mutants showed reduced binding to protein A, but not to protein G, compared with the WT IgG1, IgG2M3, and IgG4 Abs. It is notable that all of the mutants described in this study were purified by protein A chromatography with no apparent impact on yield (data not shown).

The results of this study indicate that major effector functions such as CDC and ADCC are substantially retained in IgG1 Abs engineered to have longer serum half-lives. The use of therapeutic Abs with longer serum half-lives may not only reduce the frequency of administration of such Abs in patients undergoing long-term Ab therapy but alternatively might permit the dose given to such patients to be significantly reduced. For example, assuming the serum half-life of a therapeutic Ab could be increased from ~3 to ~6 wk by introducing the T250Q/M428L mutation into the Fc, it should theoretically be possible to achieve the same steady-state trough levels of Ab in patients receiving multiple doses of the WT IgG Ab at 10 mg/kg every 4 wk by administering half the dose (i.e., 5 mg/kg) of the variant IgG at the same frequency (Fig. 8). Thus, engineered Abs with longer serum half-lives may prove to be effective therapeutics in humans.

Acknowledgments

We thank Shuang Bai, Harminder Bal, Tina Balsara, Chuck Bullock, Ferdinand Evangelista, Sharyn Farnsworth, Christine Gieswein, Catherine

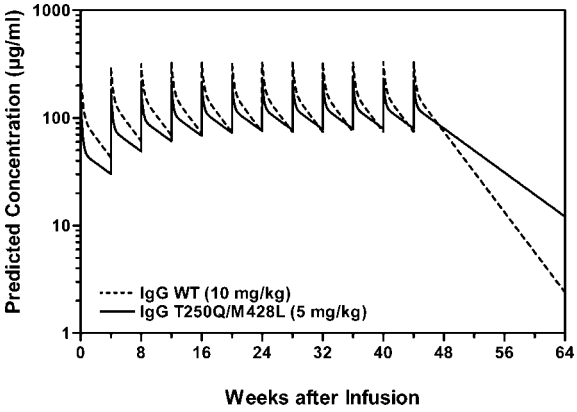

FIGURE 8. Predicted PK of OST577-IgG1 WT and mutant Abs in humans. The predicted serum Ab concentrations (μg/ml) following multiple doses of WT (10 mg/kg) or mutant (5 mg/kg) OST577-IgG1 Abs given every 4 wk by i.v. infusion were modeled assuming the WT Ab has a 3 wk half-life, and the mutant Ab has a 6 wk half-life.

Huey, Harinder Jaswal, Audrey Jia, Brett Jorgensen, Linh Le, David Maciejewski, Mauricio Maia, Julie Mikkelsen, Minha Park, Christopher Rath, Tom Robinson, Robbi Sera, Matt Sweeney, Mark Wesson, and Yin Zhang for valuable assistance and discussion. We also thank Yoshiko Akamatsu, Fiona Harding, and David Powers for comments on the manuscript and Richard Murray for support of the project.

Disclosures

P. R. Hinton, J. M. Xiong, M. T. Tang, and S. Keller are current employees, and M. G. Johlfs and N. Tsurushita are former employees, with stock or equity interests in Protein Design Labs. P. R. Hinton and N. Tsurushita are among the coinventors of pending patent applications that are assigned to Protein Design Labs.

References

1. Ghetie, V., and E. S. Ward. 2000. Multiple roles for the major histocompatibility complex class I-related receptor FcRn. *Annu. Rev. Immunol.* 18: 739–766.
2. Ghetie, V., J. G. Hubbard, J. K. Kim, M. F. Tsen, Y. Lee, and E. S. Ward. 1996. Abnormally short serum half-lives of IgG in β_2-microglobulin-deficient mice. *Eur. J. Immunol.* 26: 690–696.
3. Junghans, R. P., and C. L. Anderson. 1996. The protection receptor for IgG catabolism is the β_2-microglobulin-containing neonatal intestinal transport receptor. *Proc. Natl. Acad. Sci. USA* 93: 5512–5516.
4. Israel, E. J., D. F. Wilsker, K. C. Hayes, D. Schoenfeld, and N. E. Simister. 1996. Increased clearance of IgG in mice that lack β_2-microglobulin: possible protective role of FcRn. *Immunology* 89: 573–578.
5. Christianson, G. J., W. Brooks, S. Vekasi, E. A. Manolfi, J. Niles, S. L. Roopenian, J. B. Roths, R. Rothlein, and D. C. Roopenian. 1997. β_2-microglobulin-deficient mice are protected from hypergammaglobulinemia and have defective antibody responses because of increased IgG catabolism. *J. Immunol.* 159: 4781–4792.
6. Roopenian, D. C., G. J. Christianson, T. J. Sproule, A. C. Brown, S. Akilesh, N. Jung, S. Petkova, L. Avanessian, E. Y. Choi, D. J. Shaffer, et al. 2003. The MHC class I-like IgG receptor controls perinatal IgG transport, IgG homeostasis, and fate of IgG-Fc-coupled drugs. *J. Immunol.* 170: 3528–3533.
7. Borvak, J., J. Richardson, C. Medesan, F. Antohe, C. Radu, M. Simionescu, V. Ghetie, and E. S. Ward. 1998. Functional expression of the MHC class I-related receptor, FcRn, in endothelial cells of mice. *Int. Immunol.* 10: 1289–1298.
8. Ward, E. S., J. Zhou, V. Ghetie, and R. J. Ober. 2003. Evidence to support the cellular mechanism involved in serum IgG homeostasis in humans. *Int. Immunol.* 15: 187–195.
9. Ober, R. J., C. Martinez, C. Vaccaro, J. Zhou, and E. S. Ward. 2004. Visualizing the site and dynamics of IgG salvage by the MHC class I-related receptor, FcRn. *J. Immunol.* 172: 2021–2029.
10. Ober, R. J., C. Martinez, X. Lai, J. Zhou, and E. S. Ward. 2004. Exocytosis of IgG as mediated by the receptor, FcRn: an analysis at the single-molecule level. *Proc. Natl. Acad. Sci. USA* 101: 11076–11081.
11. Ward, E. S., C. Martinez, C. Vaccaro, J. Zhou, Q. Tang, and R. J. Ober. 2005. From sorting endosomes to exocytosis: association of Rab4 and Rab11 GTPases with the Fc receptor, FcRn, during recycling. *Mol. Biol. Cell* 16: 2028–2038.
12. Raghavan, M., V. R. Bonagura, S. L. Morrison, and P. J. Bjorkman. 1995. Analysis of the pH dependence of the neonatal Fc receptor/immunoglobulin G interaction using antibody and receptor variants. *Biochemistry* 34: 14649–14657.
13. Kim, J. K., M. F. Tsen, V. Ghetie, and E. S. Ward. 1994. Localization of the site of the murine IgG1 molecule that is involved in binding to the murine intestinal Fc receptor. *Eur. J. Immunol.* 24: 2429–2434.
14. Popov, S., J. G. Hubbard, J. Kim, B. Ober, V. Ghetie, and E. S. Ward. 1996. The stoichiometry and affinity of the interaction of murine Fc fragments with the MHC class I-related receptor, FcRn. *Mol. Immunol.* 33: 521–530.
15. Medesan, C., D. Matesoi, C. Radu, V. Ghetie, and E. S. Ward. 1997. Delineation of the amino acid residues involved in transcytosis and catabolism of mouse IgG1. *J. Immunol.* 158: 2211–2217.
16. Kim, J. K., M. F. Tsen, V. Ghetie, and E. S. Ward. 1994. Identifying amino acid residues that influence plasma clearance of murine IgG1 fragments by site-directed mutagenesis. *Eur. J. Immunol.* 24: 542–548.
17. Kim, J. K., M. F. Tsen, V. Ghetie, and E. S. Ward. 1994. Catabolism of the murine IgG1 molecule: evidence that both CH2-CH3 domain interfaces are required for persistence of IgG1 in the circulation of mice. *Scand. J. Immunol.* 40: 457–465.
18. Ghetie, V., S. Popov, J. Borvak, C. Radu, D. Matesoi, C. Medesan, R. J. Ober, and E. S. Ward. 1997. Increasing the serum persistence of an IgG fragment by random mutagenesis. *Nat. Biotechnol.* 15: 637–640.
19. Kim, J. K., M. Firan, C. G. Radu, C. H. Kim, V. Ghetie, and E. S. Ward. 1999. Mapping the site on human IgG for binding of the MHC class I-related receptor, FcRn. *Eur. J. Immunol.* 29: 2819–2825.
20. Hornick, J. L., J. Sharifi, L. A. Khawli, P. Hu, W. G. Bai, M. M. Alauddin, M. M. Mizokami, and A. L. Epstein. 2000. Single amino acid substitution in the Fc region of chimeric TNT-3 antibody accelerates clearance and improves immunoscintigraphy of solid tumors. *J. Nucl. Med.* 41: 355–362.
21. Firan, M., R. Bawdon, C. Radu, R. J. Ober, D. Eaken, F. Antohe, V. Ghetie, and E. S. Ward. 2001. The MHC class I-related receptor, FcRn, plays an essential role in the maternofetal transfer of γ-globulin in humans. *Int. Immunol.* 13: 993–1002.
22. Kenanova, V., T. Olafsen, D. M. Crow, G. Sundaresan, M. Subbarayan, N. H. Carter, D. N. Ikle, P. J. Yazaki, A. F. Chatziioannou, S. S. Gambhir, et al. 2005. Tailoring the pharmacokinetics and positron emission tomography imaging properties of anti-carcinoembryonic antigen single-chain Fv-Fc antibody fragments. *Cancer Res.* 65: 622–631.
23. Shields, R. L., A. K. Namenuk, K. Hong, Y. G. Meng, J. Rae, J. Briggs, D. Xie, J. Lai, A. Stadlen, B. Li, et al. 2001. High resolution mapping of the binding site on human IgG1 for FcγRI, FcγRII, FcγRIII, and FcRn and design of IgG1 variants with improved binding to the FcγR. *J. Biol. Chem.* 276: 6591–6604.
24. Dall'Acqua, W. F., R. M. Woods, E. S. Ward, S. R. Palaszynski, N. K. Patel, Y. A. Brewah, H. Wu, P. A. Kiener, and S. Langermann. 2002. Increasing the affinity of a human IgG1 for the neonatal Fc receptor: biological consequences. *J. Immunol.* 169: 5171–5180.
25. Gurbaxani, B., L. L. Dela Cruz, K. Chintalacharuvu, and S. L. Morrison. 2005. Analysis of a family of antibodies with different half-lives in mice fails to find a correlation between affinity for FcRn and serum half-life. *Mol. Immunol.* In press.
26. Hinton, P. R., M. G. Johlfs, J. M. Xiong, K. Hanestad, K. C. Ong, C. Bullock, S. Keller, M. T. Tang, J. Y. Tso, M. Vásquez, and N. Tsurushita. 2004. Engineered human IgG antibodies with longer serum half-lives in primates. *J. Biol. Chem.* 279: 6213–6216.
27. Ehrlich, P. H., Z. A. Moustafa, J. C. Justice, K. E. Harfeldt, R. L. Kelley, and L. Östberg. 1992. Characterization of human monoclonal antibodies directed against hepatitis B surface antigen. *Hum. Antibodies Hybridomas* 3: 2–7.
28. Co, M. S., N. M. Avdalovic, P. C. Caron, M. V. Avdalovic, D. A. Scheinberg, and C. Queen. 1992. Chimeric and humanized antibodies with specificity for the CD33 antigen. *J. Immunol.* 148: 1149–1154.
29. Yanisch-Perron, C., J. Vieira, and J. Messing. 1985. Improved M13 phage cloning vectors and host strains: nucleotide sequences of the M13mp18 and pUC19 vectors. *Gene* 33: 103–119.
30. Kostelny, S. A., B. K. Link, J. Y. Tso, M. Vásquez, B. H. Jorgensen, H. Wang, W. C. Hall, and G. J. Weiner. 2001. Humanization and characterization of the anti-HLA-DR antibody 1D10. *Int. J. Cancer* 93: 556–565.
31. Cole, M. S., C. Anasetti, and J. Y. Tso. 1997. Human IgG2 variants of chimeric anti-CD3 are nonmitogenic to T cells. *J. Immunol.* 159: 3613–3621.
32. Higuchi, R. 1989. Using PCR to Engineer DNA. In *PCR Technology: Principles and Applications for DNA Amplification.* H. A. Erlich, ed. Stockton Press, New York, pp. 61–70.
33. Kabat, E. A., T. T. Wu, H. M. Perry, K. S. Gottesman, and C. Foeller. 1991. *Sequences of Proteins of Immunological Interest.* National Institutes of Health, Bethesda, MD.
34. Sauer, P. W., J. E. Burky, M. C. Wesson, H. D. Sternard, and L. Qu. 2000. A high-yielding, generic fed-batch cell culture process for production of recombinant antibodies. *Biotechnol. Bioeng.* 67: 585–597.
35. Idusogie, E. E., L. G. Presta, H. Gazzano-Santoro, K. Totpal, P. Y. Wong, M. Ultsch, Y. G. Meng, and M. G. Mulkerrin. 2000. Mapping of the C1q binding site on rituxan, a chimeric antibody with a human IgG1 Fc. *J. Immunol.* 164: 4178–4184.
36. Koene, H. R., M. Kleijer, J. Algra, D. Roos, A. E. von dem Borne, and M. de Haas. 1997. FcγRIIIa-158V/F polymorphism influences the binding of IgG by natural killer cell FcγRIIIa, independently of the FcγRIIIa-48L/R/H phenotype. *Blood* 90: 1109–1114.
37. Morelock, M. M., R. Rothlein, S. M. Bright, M. K. Robinson, E. T. Graham, J. P. Sabo, R. Owens, D. J. King, S. H. Norris, D. S. Scher, et al. 1994. Isotype choice for chimeric antibodies affects binding properties. *J. Biol. Chem.* 269: 13048–13055.
38. West, A. P., Jr., and P. J. Bjorkman. 2000. Crystal structure and immunoglobulin G binding properties of the human major histocompatibility complex-related Fc receptor. *Biochemistry* 39: 9698–9708.

39. Tao, M. H., R. I. Smith, and S. L. Morrison. 1993. Structural features of human immunoglobulin G that determine isotype-specific differences in complement activation. *J. Exp. Med.* 178: 661–667.
40. Xu, Y., R. Oomen, and M. H. Klein. 1994. Residue at position 331 in the IgG1 and IgG4 CH2 domains contributes to their differential ability to bind and activate complement. *J. Biol. Chem.* 269: 3469–3474.
41. Morgan, A., N. D. Jones, A. M. Nesbitt, L. Chaplin, M. W. Bodmer, and J. S. Emtage. 1995. The N-terminal end of the CH2 domain of chimeric human IgG1 anti-HLA-DR is necessary for C1q, FcγRI and FcγRIII binding. *Immunology* 86: 319–324.
42. Xu, D., M. L. Alegre, S. S. Varga, A. L. Rothermel, A. M. Collins, V. L. Pulito, L. S. Hanna, K. P. Dolan, P. W. Parren, J. A. Bluestone, et al. 2000. In vitro characterization of five humanized OKT3 effector function variant antibodies. *Cell. Immunol.* 200: 16–26.
43. Hezareh, M., A. J. Hessell, R. C. Jensen, J. G. van de Winkel, and P. W. Parren. 2001. Effector function activities of a panel of mutants of a broadly neutralizing antibody against human immunodeficiency virus type 1. *J. Virol.* 75: 12161–12168.
44. Wu, J., J. C. Edberg, P. B. Redecha, V. Bansal, P. M. Guyre, K. Coleman, J. E. Salmon, and R. P. Kimberly. 1997. A novel polymorphism of FcγRIIIa (CD16) alters receptor function and predisposes to autoimmune disease. *J. Clin. Invest.* 100: 1059–1070.
45. Dall'Ozzo, S., S. Tartas, G. Paintaud, G. Cartron, P. Colombat, P. Bardos, H. Watier, and G. Thibault. 2004. Rituximab-dependent cytotoxicity by natural killer cells: influence of FCGR3A polymorphism on the concentration-effect relationship. *Cancer Res.* 64: 4664–4669.
46. Niwa, R., S. Hatanaka, E. Shoji-Hosaka, M. Sakurada, Y. Kobayashi, A. Uehara, H. Yokoi, K. Nakamura, and K. Shitara. 2004. Enhancement of the antibody-dependent cellular cytotoxicity of low-fucose IgG1 is independent of FcγRIIIa functional polymorphism. *Clin. Cancer Res.* 10: 6248–6255.
47. DeLano, W. L., M. H. Ultsch, A. M. de Vos, and J. A. Wells. 2000. Convergent solutions to binding at a protein-protein interface. *Science* 287: 1279–1283.
48. Simmons, L. C., D. Reilly, L. Klimowski, T. S. Raju, G. Meng, P. Sims, K. Hong, R. L. Shields, L. A. Damico, P. Rancatore, and D. G. Yansura. 2002. Expression of full-length immunoglobulins in *Escherichia coli*: rapid and efficient production of aglycosylated antibodies. *J. Immunol. Methods* 263: 133–147.
49. Tao, M. H., and S. L. Morrison. 1989. Studies of aglycosylated chimeric mouse-human IgG. Role of carbohydrate in the structure and effector functions mediated by the human IgG constant region. *J. Immunol.* 143: 2595–2601.
50. Dorai, H., B. M. Mueller, R. A. Reisfeld, and S. D. Gillies. 1991. Aglycosylated chimeric mouse/human IgG1 antibody retains some effector function. *Hybridoma* 10: 211–217.
51. Horan Hand, P., B. Calvo, D. Milenic, T. Yokota, M. Finch, P. Snoy, K. Garmestani, O. Gansow, J. Schlom, and S. V. Kashmiri. 1992. Comparative biological properties of a recombinant chimeric anti-carcinoma mAb and a recombinant aglycosylated variant. *Cancer Immunol. Immunother.* 35: 165–174.
52. Routledge, E. G., M. E. Falconer, H. Pope, I. S. Lloyd, and H. Waldmann. 1995. The effect of aglycosylation on the immunogenicity of a humanized therapeutic CD3 monoclonal antibody. *Transplantation* 60: 847–853.
53. Ferrant, J. L., C. D. Benjamin, A. H. Cutler, S. L. Kalled, Y. M. Hsu, E. A. Garber, D. M. Hess, R. I. Shapiro, N. S. Kenyon, D. M. Harlan, et al. 2004. The contribution of Fc effector mechanisms in the efficacy of anti-CD154 immunotherapy depends on the nature of the immune challenge. *Int. Immunol.* 16: 1583–1594.
54. Wright, A., Y. Sato, T. Okada, K. H. Chang, T. Endo, and S. L. Morrison. 2000. In vivo trafficking and catabolism of IgG1 antibodies with Fc associated carbohydrates of differing structure. *Glycobiology* 10: 1347–1355.
55. Wright, A., and S. L. Morrison. 1998. Effect of C2-associated carbohydrate structure on Ig effector function: studies with chimeric mouse-human IgG1 antibodies in glycosylation mutants of Chinese hamster ovary cells. *J. Immunol.* 160: 3393–3402.
56. Martin, W. L., A. P. West, Jr., L. Gan, and P. J. Bjorkman. 2001. Crystal structure at 2.8 Å of an FcRn/heterodimeric Fc complex: mechanism of pH-dependent binding. *Mol. Cell* 7: 867–877.
57. Deisenhofer, J. 1981. Crystallographic refinement and atomic models of a human Fc fragment and its complex with fragment B of protein A from *Staphylococcus aureus* at 2.9- and 2.8-Å resolution. *Biochemistry* 20: 2361–2370.
58. Saphire, E. O., R. L. Stanfield, M. D. Crispin, P. W. Parren, P. M. Rudd, R. A. Dwek, D. R. Burton, and I. A. Wilson. 2002. Contrasting IgG structures reveal extreme asymmetry and flexibility. *J. Mol. Biol.* 319: 9–18.
59. Idusogie, E. E., P. Y. Wong, L. G. Presta, H. Gazzano-Santoro, K. Totpal, M. Ultsch, and M. G. Mulkerrin. 2001. Engineered antibodies with increased activity to recruit complement. *J. Immunol.* 166: 2571–2575.
60. Boyd, P. N., A. C. Lines, and A. K. Patel. 1995. The effect of the removal of sialic acid, galactose and total carbohydrate on the functional activity of Campath-1H. *Mol. Immunol.* 32: 1311–1318.
61. Mimura, Y., S. Church, R. Ghirlando, P. R. Ashton, S. Dong, M. Goodall, J. Lund, and R. Jefferis. 2000. The influence of glycosylation on the thermal stability and effector function expression of human IgG1-Fc: properties of a series of truncated glycoforms. *Mol. Immunol.* 37: 697–706.
62. Cartron, G., L. Dacheux, G. Salles, P. Solal-Celigny, P. Bardos, P. Colombat, and H. Watier. 2002. Therapeutic activity of humanized anti-CD20 monoclonal antibody and polymorphism in IgG Fc receptor FcγRIIIa gene. *Blood* 99: 754–758.
63. Anolik, J. H., D. Campbell, R. E. Felgar, F. Young, I. Sanz, J. Rosenblatt, and R. J. Looney. 2003. The relationship of FcγRIIIa genotype to degree of B cell depletion by rituximab in the treatment of systemic lupus erythematosus. *Arthritis Rheum.* 48: 455–459.
64. Weng, W. K., and R. Levy. 2003. Two immunoglobulin G Fc receptor polymorphisms independently predict response to rituximab in patients with follicular lymphoma. *J. Clin. Oncol.* 21: 3940–3947.
65. Treon, S. P., M. Hansen, A. R. Branagan, S. Verselis, C. Emmanouilides, E. Kimby, S. R. Frankel, N. Touroutoglou, B. Turnbull, K. C. Anderson, et al. 2005. Polymorphisms in FcγRIIIA (CD16) receptor expression are associated with clinical response to rituximab in Waldenstrom's macroglobulinemia. *J. Clin. Oncol.* 23: 474–481.
66. Sauer-Eriksson, A. E., G. J. Kleywegt, M. Uhlén, and T. A. Jones. 1995. Crystal structure of the C2 fragment of streptococcal protein G in complex with the Fc domain of human IgG. *Structure* 3: 265–278.